https://dx.doi.org/10.1016/j.jclepro.2023.140343

Sustainable Microwave-heating Healing Asphalt Concrete Fabricated with Waste Microwave-sensitive Fillers

Dong Lu [a,b], Xi Jiang [a,*], Zhen Leng [a,*]

[a] *Department of Civil and Environmental Engineering, The Hong Kong Polytechnic University, Hong Kong SAR*

[b] *School of Civil Engineering, Harbin Institute of Technology, Harbin, 150090, PR China*

***Corresponding Authors**: Xi Jiang, xi.jiang@polyu.edu.hk; Zhen Leng, zhen.leng@polyu.edu

Abstract

The use of waste fillers as substitutes for limestone powder (LP) filler is a promising way to consume industrial by-products and achieve sustainable asphalt pavement. This study recycles three types of microwave-sensitive fillers, namely, coal gangue powder (CGP), ferrite powder (FP), and fly ash (FA), as alternatives to LP filler, in the creation of microwave-heating healing asphalt composites. The results indicate that conventional LP-modified asphalt mastics have a self-healing initiation temperature of 88.2℃. On the contrary, CGP-modified asphalt mastics and FP-modified asphalt mastics exhibit significantly lower starting self-healing temperatures, with values of 65.6℃ and 56.2℃, respectively. Moreover, CGP-modified asphalt mastics and FP-modified asphalt mastics achieve an average surface temperature surpassing 95℃ within 60 seconds of microwave heating. It is worth noting that FP-modified asphalt mastics retain an impressive healing index of 46.6% even after three cycles of damage-healing-damage. The incorporation of microwave-sensitive fillers in asphalt composites can improve the conversion efficiency of microwave radiation to thermal energy, and thus enhance the microwave-heating healing characteristics compared to conventional LP-modified asphalt composites. Additionally, a comprehensive assessment of the environmental benefits and economic costs reveals significant cost savings and reductions in CO_2 emissions associated with the adoption of microwave-heating healing asphalt pavement. These findings strongly support the practical implementation of microwave-sensitive fillers in asphalt composites, leading to improved maintenance efficiency, enhanced serviceability, and sustainability for pavement systems.

Keywords: Asphalt concrete; Solid waste recycling; Waste filler; Microwave-heating healing; Sustainable pavement

Abbreviations

LP, Limestone powder; CGP, Coal gangue powder; FP, Ferrite powder; FA, Fly ash, PG, Performance grading; PA, Porous asphalt; XRF, X-ray fluorescence; DSR, Dynamic shear rheometer; SCB, Semi-circular bending; HI, Healing index; EBEC, Environmental benefits and economic cost.

1. Introduction

Asphalt mixture has been extensively utilized in pavement construction due to the benefits of mechanized construction, low cost, and driving comfort (Ma et al., 2021; Segundo et al., 2021). However, throughout its lifespan, the asphalt mixture is exposed to diverse natural and human factors, including sunlight, rainfall, and vehicular load, which can result in various forms of damage (Grossegger and Garcia, 2019; Lu et al., 2023a; Ma et al., 2022b). Damage in asphalt pavement typically begins as microcracks and progresses to macroscopic cracks, causing a range of detrimental effects (Lu et al., 2023c; Santero et al., 2011; Varma et al., 2021). These damages can significantly impact the durability of the pavement and pose safety risks for drivers (Jahanbakhsh et al., 2018). Therefore, it is crucial to heal these microcracks, ideally in their early stages, to prevent further propagation and widening. The objective of healing these microcracks is to restore the performance of the asphalt mixture efficiently and cost-effectively, ultimately extending the lifespan of the pavement.

It is widely recognized that asphalt binder has inherent self-healing behavior, with certain microcracks capable of repairing themselves under intermittent loading conditions (García, 2012; Mehrara and Khodaii, 2015). This behavior is attributed to the thermodynamic movements of asphalt molecules, such as infiltration, diffusion, and dissolution (García et al., 2013). Notably, raising the temperature with the aid of external energy can speed up the migration of asphalt molecules (Amani et al., 2020; Liu et al., 2013). Therefore, it is crucial to employ auxiliary heating techniques to elevate the asphalt temperature and improve its self-healing capability (Anupam et al., 2022; Varma et al., 2021; Xu et al., 2018).

Previous studies have confirmed that microwave radiation is an efficient and environmentally friendly heating method to enhance the healing efficiency of asphalt materials as compared to the electromagnetic induction heating technique, and it has been widely used in recent decades (Liu et al., 2022; M. Karimi et al., 2022; Zhu et al., 2019). Typically, microwave-sensitive additives, such as metal-based fibers (Schuster et al., 2023) or carbon-based materials (Jahanbakhsh et al., 2018; Karimi et al., 2018), are directly mixed with asphalt before mixing with aggregate and filler to make self-healing asphalt materials. However, achieving proper dispersion of these additives within the asphalt remains a significant challenge, and the pre-dispersion treatment is time-consuming and expensive (Wang et al., 2016; Wang et al., 2022; Wen and Chung, 2004). Moreover, the aggregation of the additives can result in localized overheating under microwave radiation, which may cause the asphalt mixture to collapse (Karimi et al., 2021). Another promising approach to enhance the efficiency of microwave-heating healing in asphalt mixtures involves

the incorporation of steel or iron slag as a partial replacement for natural aggregate (Yang et al., 2022b). However, this method may result in concentrated heating and durability concerns (Liu et al., 2022). Moreover, the unstable properties of solid waste materials like steel or iron slag and their associated transportation costs pose practical limitations on their application (Jiang, Q. et al., 2023; Jiang et al., 2018; Song, Q. et al., 2021; Yang et al., 2022a). Given these limitations, it is evident that the development of effective and precise techniques for microwave-heating healing in asphalt mixtures is crucial.

Recent studies have highlighted the potential of coal gangue powder (CGP), ferrite powder (FP), and fly ash (FA) in improving the rheological properties, rutting resistance, and cracking resistance of asphalt materials, presenting a viable alternative to limestone powder (LP) (Li et al., 2023; Li et al., 2022; Muhammad et al., 2021; Nabiun and Khabiri, 2016; Woszuk et al., 2019). Moreover, these fillers contain a significant amount of metallic oxides and exhibit excellent microwave absorption capabilities (Lu et al., 2023b; Norambuena-Contreras and Garcia, 2016). When exposed to microwave radiation, they can generate heat, making them an environmentally friendly and cost-effective choice for microwave heating and healing in asphalt materials. While microwave-sensitive fillers show promise for use in microwave heating-healing asphalt materials, comprehensive studies on their efficacy as substitutes for LP are lacking. Additionally, there is limited literature available comparing the effectiveness of different microwave-sensitive fillers for the microwave-heating healing behavior of asphalt materials. As such, further research and investigation are needed to fully understand the potential of these fillers and their performance in enhancing the microwave-heating healing characteristics of asphalt materials.

To bridge the research gap and advance the practical applications of microwave-heating healing asphalt materials, this study aims to utilize industrial by-products such as CGP, FP, and FA as substitutions for LP filler for developing sustainable microwave-heating healing asphalt materials. To assess their potential for practical applications, the rutting factor, microwave heating ability, and microwave-heating healing behavior of asphalt materials are systematically evaluated in this research. The findings of this research hold promising implications for the practical use of microwave-sensitive filler-modified asphalt materials, paving the way for improved maintenance efficiency and serviceability and offering opportunities to achieve sustainable pavements.

2. Experimental

2.1. Materials

The asphalt used in this study is PG-76/22 and its main properties are provided in **Table S1** (Supporting Information). To increase the microwave-heating property of asphalt materials, three microwave-sensitive fillers, namely CGP, FP, and FA, were used as substitutes for LP filler. The fundamental properties of these four fillers are presented in **Table 1**. Importantly, the particle sizes of these microwave-sensitive fillers are similar to those of the LP, eliminating the need for additional pre-dispersing processes. The microwave-heating healing property of the asphalt materials was evaluated by employing a porous asphalt (PA) mixture, with a nominal maximum aggregate dimension of 13.2 mm (PA-13). **Table S2** (Supporting Information) presents the aggregate gradation used for preparing the PA mixture.

Table 1 Basic properties of four types of fillers.

Properties	LP	CGP	FP	FA
Density (g/cm^3)	2.556	2.643	5.120	2.860
Specific surface area (m^2/g)	0.23	0.27	2.16	3.69

2.2. Preparation of asphalt materials

As shown in **Table 2**, a volume control method was adopted to maintain consistent volume composition of different asphalt mastic specimens. **Fig. 1** illustrates the experimental setup and process, where the asphalt was initially heated in a sample vessel maintained at a temperature of 170℃. Subsequently, the filler was heated to 180℃ for 60 minutes before being mixed with the asphalt binder. The filler-binder ratio was kept at 1.0 throughout the experiments. Homogeneous dispersion of the filler in the asphalt was achieved using an ESK-500 high-speed shearing machine at 1800 r/min for 30 minutes.

To assess the microwave-heating healing efficiency of asphalt composites, PA-13 mixture was prepared. The optimum asphalt content and filler content were determined to be 3.9% and 1.5 wt% by weight of the asphalt mixture. The LP filler was replaced by the functional fillers in an equivalent volume. The preparation process involved dry mixing the aggregates for 60 seconds, followed by mixing them with the asphalt for 90 seconds. Subsequently, the filler was introduced into the mixture and mixed for another 90 seconds. The well-mixed mixture was finally compacted using a rotary compaction machine. The obtained standard Marshall specimens were cut into semi-circular specimens (diameter=150 mm, thickness=50 mm,

and height=75 mm) for semi-circular bending (SCB) bending tests.

Table 2 Mix ratios of asphalt mastics.

Sample ID	Mix ratio of fillers (%)				Filler-Binder ratio
	LP	CGP	FP	FA	
AM-LP	100	0	0	0	1.0
AM-CGP	0	100	0	0	
AM-FP	0	0	100	0	
AM-FA	0	0	0	100	

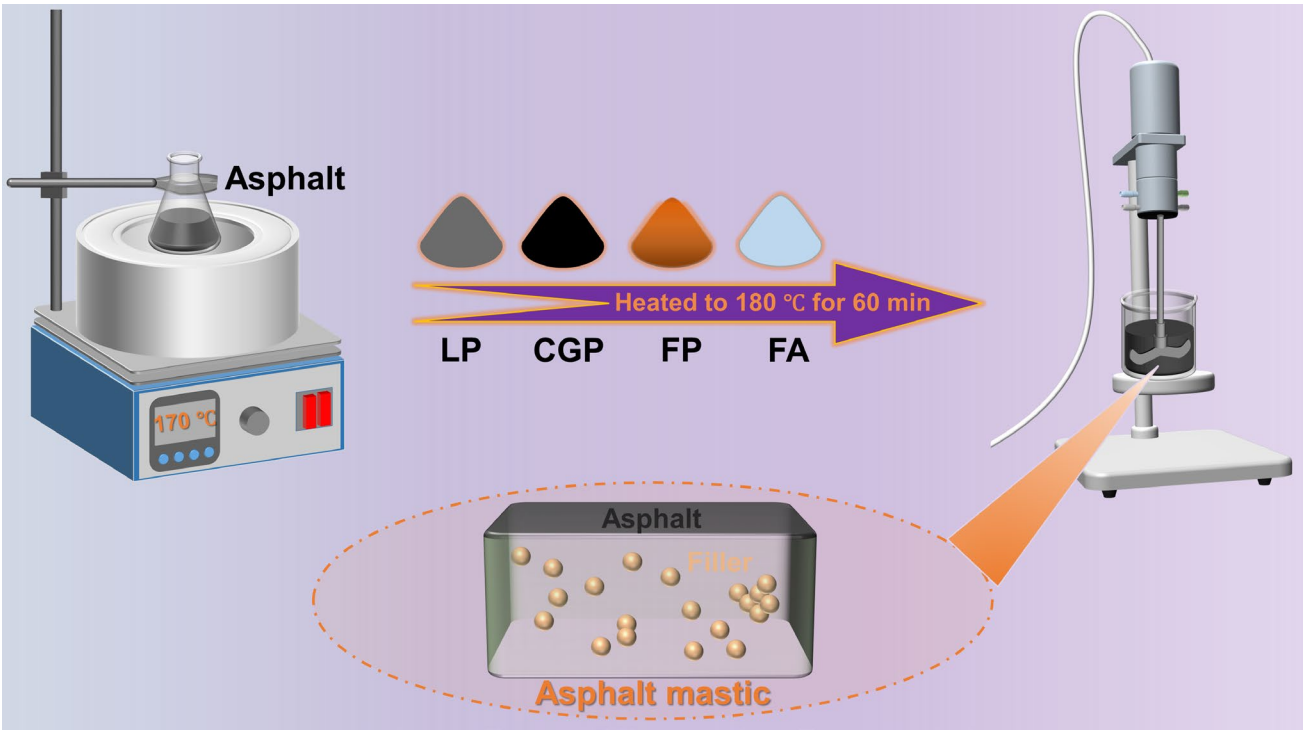

Fig. 1. Illustration of preparation of asphalt mastics. LP is Limestone powder; CGP is Coal gangue powder; FP is Ferrite powder; and FA is Fly ash.

2.3. Test programs

2.3.1. Properties of filler

The morphology of the fillers was acquired through scanning electron microscopy (SEM). Before observation, the fillers were oven-dried and then sputter-coated with a gold (Au) film. The resulting samples

were then subjected to SEM analysis to examine their morphology. Furthermore, the fillers' chemical compositions were examined through an X-ray fluorescence (XRF) spectrometer with a power and current of 4 kW and 160 mA, respectively, enabling accurate determination of the fillers' compositions.

The real parts and imaginary parts of the complex permittivity and relative complex permeability of the fillers were determined using a microwave vector network analyzer system (AGILENT, PNA-N5244A) through coaxial transmission/reflection measurements. A frequency of 1-18 GHz was applied in this study, as recommended by our previous study (Liu et al., 2023). To facilitate the measurement process, paraffin wax was utilized as a bonding agent to form the samples. Paraffin wax does not exhibit any microwave absorption. The mixing weight ratio of filler to paraffin was 1:1 to ensure proper adhesion between filler and paraffin, allowing for accurate measurement of the electromagnetic parameters of the fillers.

2.3.2. Rutting factor

An Anton Paar CTD 180 Dynamic Shear Rheometer (DSR) was employed to access the high-temperature rheological property of the asphalt mastics using a temperature scanning mode. Two temperature tests were performed at 82℃ and 88℃, both at a scanning frequency of 10 rad/s and a 0.1% strain amplitude, as recommended by previous studies (Meng et al., 2023; Zhou et al., 2022). This strain amplitude value helps maintain the asphalt mastic's rheological property in a range where it exhibits linear viscoelastic properties.

2.3.3. Microwave heating properties

To measure the heating rate, approximately 2 ml of each group of asphalt mastic samples were weighed. These samples were then put on a plastic plate for microwave heating. The samples were heated using a microwave oven with a power output of 800 W. Each sample was subjected to continuous radiation for 3 minutes, with heating intervals of 30 seconds each. After each heating interval, the temperature of the samples was recorded through an infrared thermal imager (FLIR T650sc). The initial temperature of the mastics, represented as T_0, was recorded at room temperature. The microwave-heating rate (V_H, ℃/s) of the asphalt mastics was determined using **Equation (1)**:

$$V_H = \frac{T - T_0}{t} \quad (1)$$

where T_0 represents the initial temperature of the mastics, T represents the temperature of the mastics after heating (℃), respectively, and t is the microwave radiation duration (s).

2.3.4. Microwave-heating healing behavior

The microwave-assisted healing behavior of asphalt materials is significantly influenced by temperature, as the asphalt molecules possess the ability to effectively repair microcracks when the sample reaches its designated self-healing temperature (Tan et al., 2012). As a viscoelastic material, asphalt demonstrates liquid-like characteristics at elevated temperatures (García, 2012). Previous study has recommended determining the initial self-healing temperature of asphalt materials is related to their viscous flow properties, using the relationship between frequency and complex viscosity (Liu et al., 2021). To establish this relationship, a frequency sweep mode was conducted using a CTD 180 DSR, as depicted in **Fig. 2a**. A dynamic scanning frequency of 0.1 Hz-100 Hz at different temperatures (40℃, 55℃, 70℃, 85℃, 100℃) was performed in this study. The viscous flow behavior of the asphalt mastics can be fitted using **Equation 2**, according to the scanning frequency and viscosity data.

$$\eta * = m|f|^{n-1} \tag{2}$$

where η^* is complex viscosity; f is scanning frequency; m and n are the fitting parameters, n represents the flow behavior value. Typically, asphalt can be viewed as a near-Newtonian fluid as its flow behavior index is 0.9-1.0. As such, the temperature at which n equals 0.9 is considered to be the temperature at which the asphalt mastic reaches initial healing.

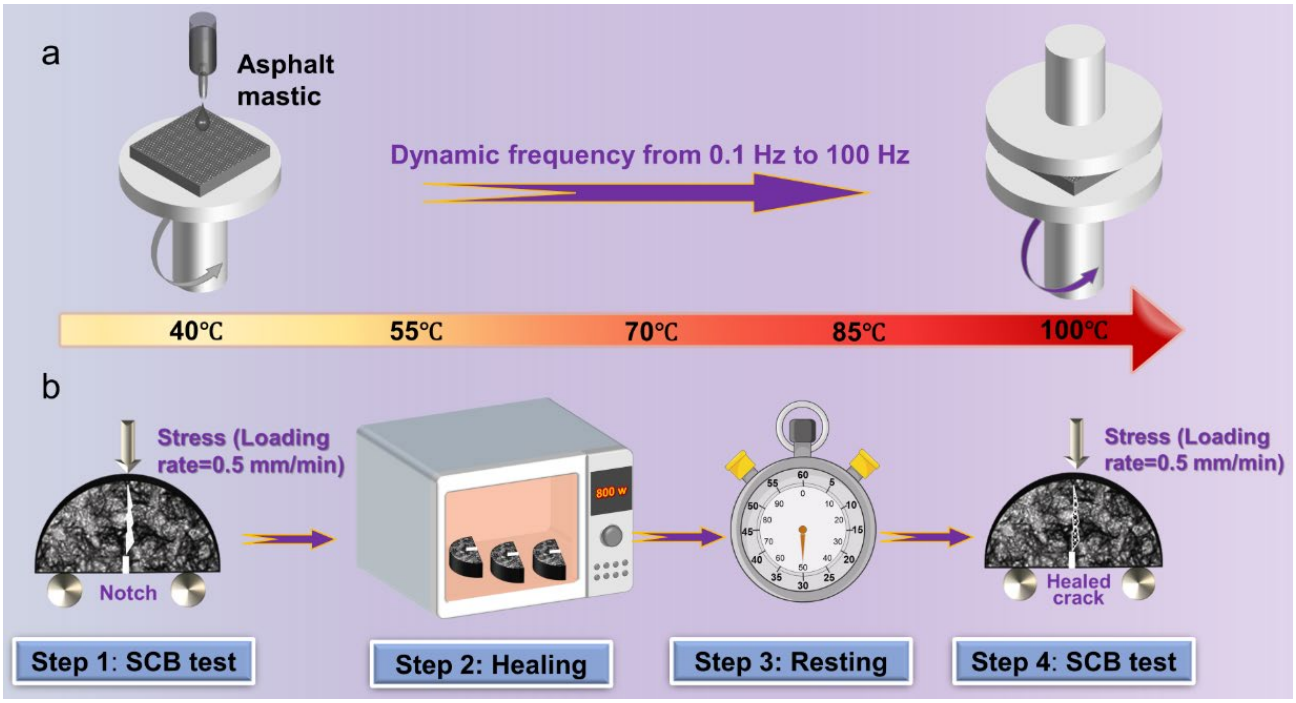

Fig. 2. The procedure of heating-healing properties of asphalt materials: (a) frequency sweep and (b) the damage-healing-damage tests of asphalt mixtures.

As recommended by previous literature (Jahanbakhsh et al., 2018; Song et al., 2023b), the SCB test offers advantages such as low cost, simple sample preparation, and a straightforward testing setup. Consequently, it has been widely used for characterizing the cracking resistance and self-healing properties of asphalt concrete (Karimi et al., 2018; Song et al., 2023a; Song, W. et al., 2021). According to our previous study (Lu et al., 2023b), a damage-healing-damage test was conducted to assess the microwave-heating healing capability of the asphalt mixture. As shown in **Fig. 2b**, SCB tests were performed to intentionally create a small crack (1.5 mm in width and 15 mm in height), resulting in a damaged sample. The damaged samples were then reassembled and exposed to microwave heating at 800 W for different durations. Afterwards, allow them to rest at ambient temperature for 6 hours. Finally, the samples underwent another SCB bending test, finishing a cycle. The healing index (*HI*, %) of the asphalt mixture is defined as the relationship between the peak force measured in the samples after healing and the initial peak force of the samples during a SCB test (García, 2012), which was calculated through **Equation** (3):

$$HI=F_1/F_0\times100\% \quad (3)$$

where F_0 is the peak force initially tested and F_1 is the peak force of the specimens after healing (N).

3. Results and discussion

3.1. Characterization of filler properties

In this section, the morphology, chemical compositions, microwave absorption behavior, and microwave heating capability of the four types of fillers are analyzed and compared.

3.1.1. Morphology and chemical compositions

As suggested in **Fig. 3a**, the LP exhibits a grey-white appearance and has a flat surface as observed under SEM observation. **Fig. 3b** shows that CGP has a dark-brown color because of the high content of coal. Additionally, the surface of the CGP is rough and has visible protrusions and wrinkles, as well as an abundant pore structure, primarily attributed to carbon volatilization. These unique characteristics enhance the ability of CGP to absorb more asphalt film and significantly increase the contact region between filler and asphalt. As a result, CGP-asphalt demonstrates improved bonding strength relative to that of the LP-asphalt (Hong et al., 2020). As shown in **Fig. 3c**, FP exhibits a red-brown appearance, and its SEM image reveals a plate-shaped structure with a thickness of several micrometers and a length of approximately 20 micrometers. This morphology allows FP to contribute to the improved performance of the asphalt binder

when mixed together. **Fig. 3d** shows that FA has a grey appearance and a perfect spherical structure. This unique structure facilitates the easy mixing of FA with asphalt binder, further enhancing the compatibility between the two materials, which has been discussed in our previous study (Lu et al., 2023e). XRF results presented in **Fig. 3e** indicate that the LP contains a high content of CaO, reaching as high as 95.4%. In contrast, as shown in **Fig. 3f-Fig. 3h**, CGP, FP, and FA possess higher contents of metal oxides, such as Fe_2O_3, Al_2O_3, and ZnO, when compared to LP. This higher metal oxide content contributes to their efficiency in absorbing microwave energy and ensuring rapid microwave heating of asphalt materials, as previously observed in recent studies (Guan et al., 2019; Li et al., 2022).

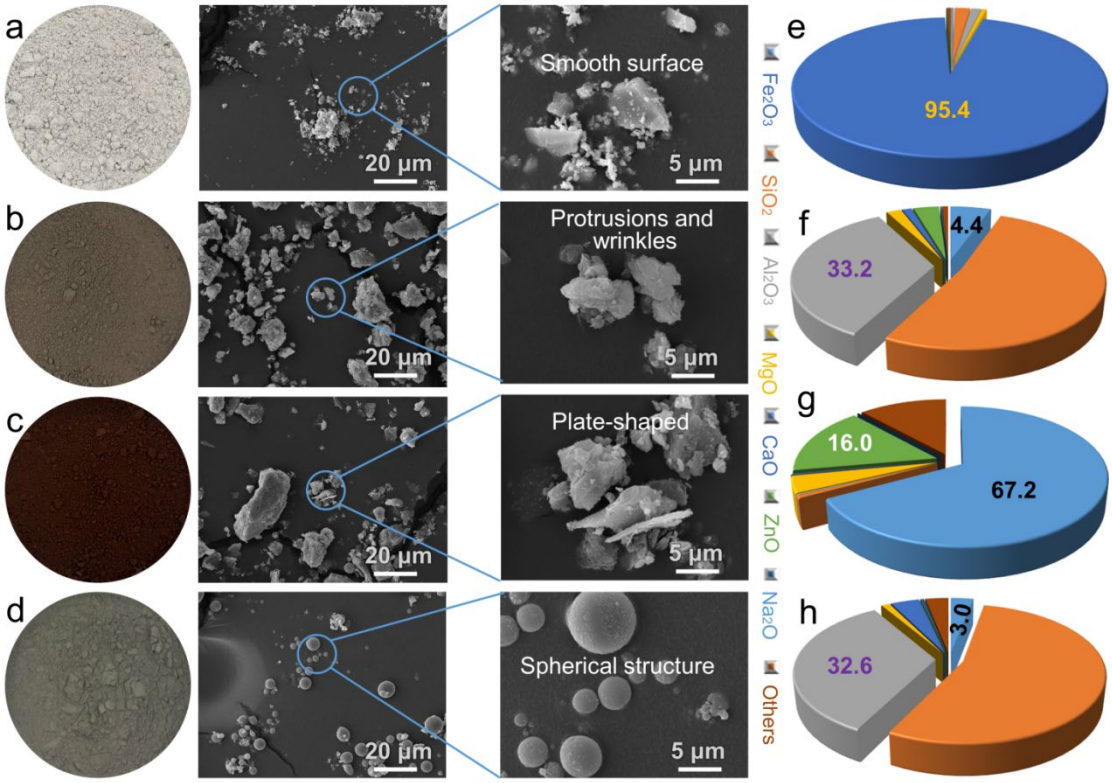

Fig. 3. Morphology and components of fillers: appearance and SEM images of (a) LP; (b) CGP; (c) FP; and (d) FA; chemical compositions of (e) LP; (f) CGP; (g) FP; and (h) FA.

3.1.2. Microwave absorption behavior

Previous studies (Li et al., 2018; Lou et al., 2020) have explored the heating mechanism of asphalt materials subjected to microwave irradiation and have identified two key aspects: 1) Absorption of microwave energy by the microwave-sensitive fillers: Fillers in asphalt materials have distinct electromagnetic parameters and structures, leading to differences in their reflection loss. This variance in reflection loss allows fillers to effectively absorb microwave energy, leading to the attenuation of

microwave absorption (Li et al., 2018); and 2) Conversion of microwave energy into heat via the "internal friction heat" mechanism, mainly attributed to the dipole molecules' high-frequency reciprocating motion within the filler, which generates heat and raises the temperature of the asphalt materials (Liu et al., 2023). The electromagnetic parameters, namely, relative complex permittivity and relative complex permeability, along with their real and imaginary parts, indicate the storage capacity and loss capability of microwave energy by the fillers (Li et al., 2018).

In **Fig. 4**, the real part of the complex permittivity of all mastic groups exhibits a fluctuating pattern, while the imaginary part tends to have lower values (bottom rows in **Fig. 4a** and **Fig. 4b**). The LP, due to its insensitivity to microwave radiation, demonstrates a real part of the complex permittivity ranging between 2.8-3.0 and an imaginary part ranging between 0.1-0.4. These values indicate lower dielectric parameters, resulting in inadequate microwave heating and healing properties for AM-LP samples (this will be elaborated in section 3.1.3). In contrast, CGP, FP, and FA samples exhibit significantly higher values for the real and imaginary parts of the complex permittivity compared to LP samples. This suggests that these three types of fillers have the potential to be excellent microwave absorbers with significant magnetic loss capabilities. The abundance of magnetic components within these fillers is mainly responsible for their enhanced microwave absorption properties.

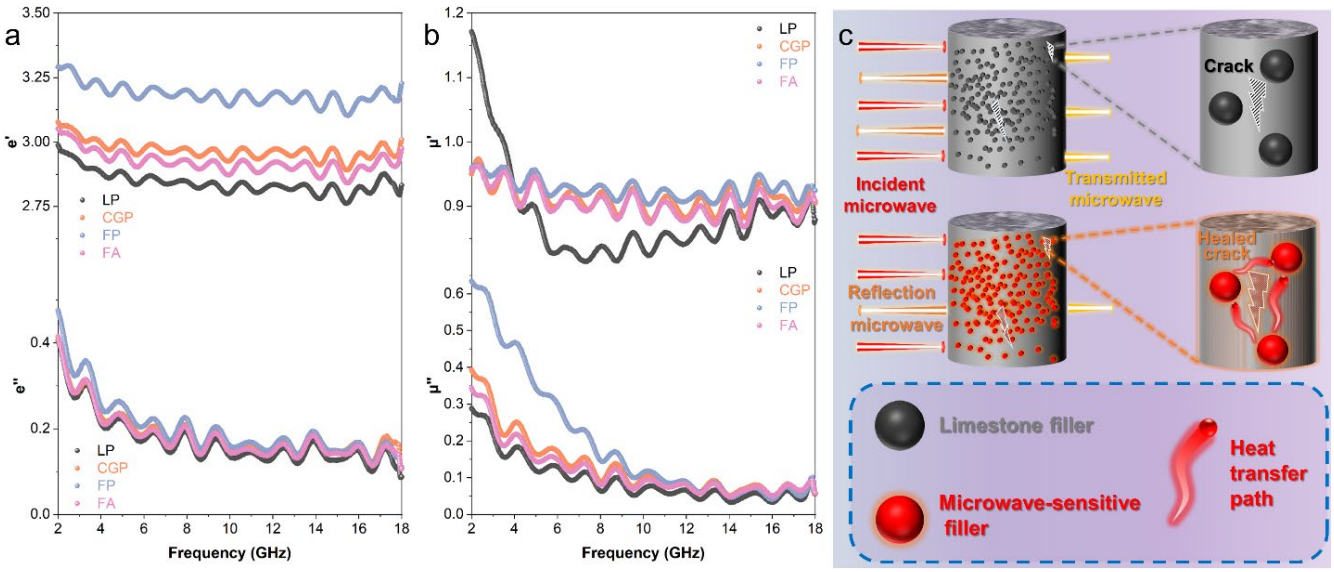

Fig. 4. Microwave absorption of fillers: (a) real parts (up) and imaginary parts (bottom) of the complex permittivity; and (b) real parts (up) and imaginary parts (bottom) of the relative complex permeability.; and (c) illustration of different forms of microwaves in asphalt materials under microwave radiation.

As illustrated in **Fig. 4c,** under microwave irradiation, asphalt materials incorporating microwave-sensitive fillers, such as CGP, FP, or FA demonstrate higher imaginary parts of relative complex permittivity and relative complex permeability. Consequently, these composites exhibit an increased ability to efficiently convert microwave energy into heat release. This heat release is induced by electric loss, which encompasses conduction loss and dielectric loss, involving the polar orientation and displacement of electric dipoles within the asphalt materials (Li et al., 2018). Additionally, asphalt composites modified with LP show lower heating-healing efficiency due to their inferior capacity to transfer microwave energy into heat. Therefore, the inclusion of CGP, FP, or FA in asphalt materials can enhance the effectiveness of microwave-induced heating and healing processes.

3.1.3. Microwave heating capability

In **Fig. 5**, the heating ability of four different fillers when subjected to microwave radiation is analyzed and compared. As expected, all fillers' surface temperature enhances with the duration of microwave heating. In the case of LP, the average surface temperature only reaches 34.5℃ and 64℃ after 60 seconds and 180 seconds of microwave heating, respectively. However, the microwave-sensitive fillers exhibit significantly higher temperatures compared to the LP sample at any given duration of microwave radiation. Specifically, after 60 seconds of microwave radiation, the average surface temperature of CGP, FP, and FA rises rapidly to 96℃, 104℃, and 73.1℃, respectively. Notably, PG 76/22's softening point is approximately 95℃ (see **section 2.1**), which implies that the surface temperatures of CGP and FP after 60 seconds of microwave heating are sufficient to soften asphalt binder. These findings suggest that microwave-sensitive fillers, particularly CGP and FP, possess exceptional heat formation capabilities with the assistance of microwave heating and hold significant potential for softening the surrounding binder.

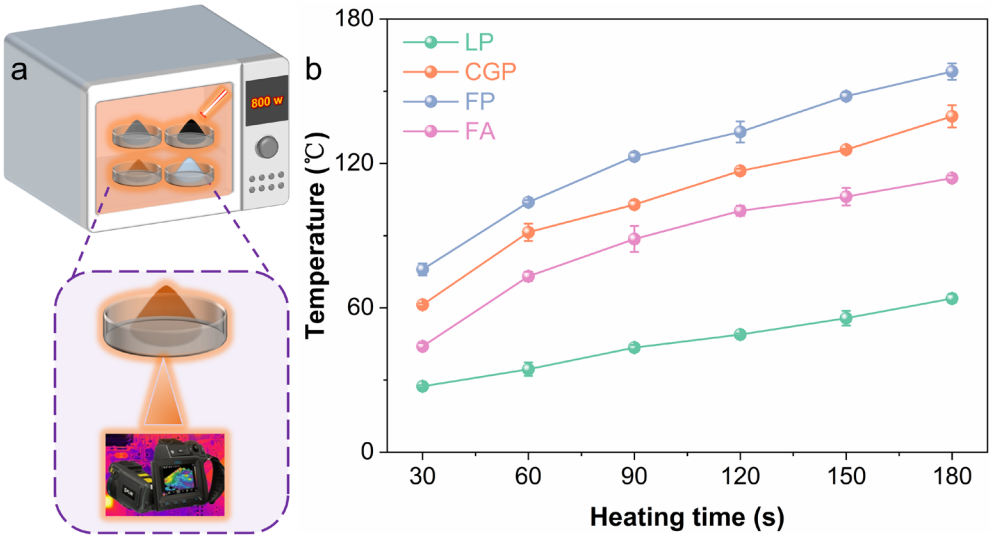

Fig. 5. Fillers' microwave heating ability: (a) illustration of fillers subjected to microwave radiation and (b) surface temperatures of fillers within 180 seconds.

The microwave-sensitive fillers typically have a higher content of metal oxides, exhibit the ability to generate heat more efficiently and facilitate uniform heat transfer in asphalt materials (Lu et al., 2023d; Wan et al., 2022; Zhu et al., 2019). Remarkably, significant heat formation and uniform heat transfer can be achieved in just 60 seconds of microwave radiation when using these fillers, surpassing the performance of LP. This suggests that replacing LP with microwave-sensitive fillers is a promising way to greatly improve the heating-healing capabilities of asphalt materials. Furthermore, such a substitution could also bring about potential environmental and economic benefits.

3.2. Rutting factor of asphalt mastics

The observed trend in the rutting factor values of all samples aligns with expectations, as they decrease as the temperature increases. This decline signifies a reduced resistance to permanent deformation in asphalt mastics as the temperature rises (as depicted in **Fig. 6a**). Moreover, the rutting factors of the AM-CGP, AM-FP, and AM-FA samples surpass that of the AM-LP, indicating that these fillers have the potential to enhance the hardness and rutting resistance of asphalt mastics, mainly attributed to the higher density of microwave-sensitive fillers in comparison to LP, as mentioned in section 2.1. In addition to their higher density, microwave-sensitive fillers also possess a higher specific surface area. This increased surface area facilitates greater contact with the asphalt binder. The SEM images of the asphalt mastics provide further evidence for this, as the microwave-sensitive fillers exhibit rough and porous surfaces that can absorb more free asphalt within the mastic. This absorption limits the flow of asphalt, contrasting with LP's flat and

smooth surfaces. By acting as a filled skeleton, the incorporated microwave-sensitive fillers can enhance the interfaces between the asphalt and fillers. This improvement allows the asphalt mastics to better withstand shear forces, ultimately increasing their rigidity.

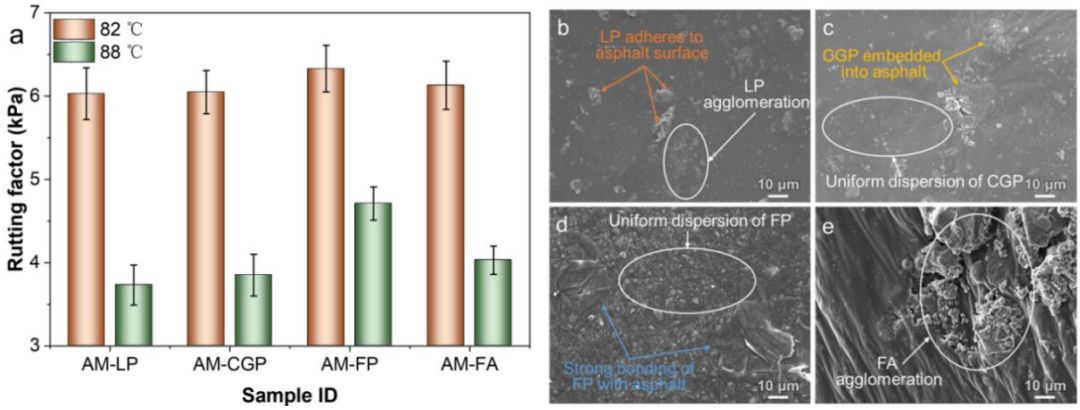

Fig. 6. (a) Rutting factor of asphalt mastics; SEM images of (b) AM-LP; (c) AM-CGP; (d) AM-FP; and (e) AM-FA samples.

Based on the findings depicted in **Fig. 6b**, the admixing LP filler and asphalt do not establish sufficient contact.. In contrast, CGP interacts strongly with the asphalt, leading to a blurred interface. This indicates that CGP has better adhesion to the asphalt interface (as depicted in **Fig. 6c**). Additionally, the dispersion of CGP throughout the asphalt mixture appears to be relatively homogeneous. The incorporation of FP results in a decrease in fractional voids, as observed in **Fig. 6d**. Moreover, the AM-FP sample exhibits improved and more uniform bonding with the asphalt. This improvement can be attributed to the smaller granulometry of FP compared to LP. In **Fig. 6e**, significant agglomeration of FA particles is observed, and the asphalt encapsulates the FA particles. Although voids remain due to the hollow and porous particle characteristics of FA, the asphalt-filler bonding may not be as strong. Additionally, the hydrophilic nature of FA poses challenges in achieving proper mixing with the asphalt due to its high viscosity. Note that the possible aggregation of microwave-sensitive fillers could result in localized overheating inside the asphalt mastics during microwave radiation. As such, addressing this issue is crucial before considering the practical applications of this technology.

3.3. Microwave heating behavior of asphalt mastics

The surface temperature distribution of the asphalt mastics can be measured in a non-contact and real-time manner using infrared cameras. As depicted in **Fig. 7**, the majority of regions in the AM-LP sample achieve approximately 45°C after 90 seconds of microwave heating. This temperature level does not

achieve the temperature required for softening the surrounding asphalt. Microwave-sensitive fillers modified asphalt mastics exhibit a surface that is covered with red and bright colors, particularly in the case of the AM-CGP and AM-FP samples. These samples demonstrate the highest surface temperatures of around 95℃ and 110℃, respectively, at 90 seconds. This indicates that the AM-CGP and AM-FP samples possess excellent microwave thermal heating rates and uniformity. However, the AM-FA sample exhibits relatively low-efficiency microwave heating capability, likely due to its limited metal oxide components. Notably, the temperature over 100℃ may lead to asphalt deterioration after 120 seconds. Therefore, in practical applications, the duration of microwave radiation should be appropriately controlled to prevent excessive heating.

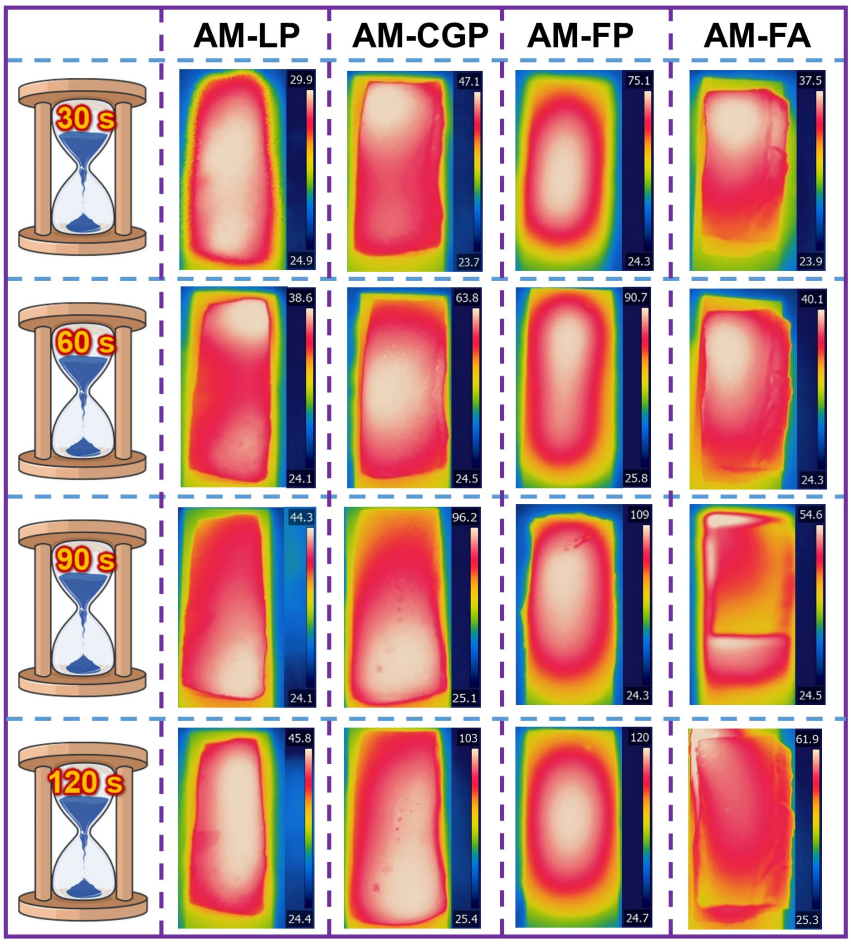

Fig. 7. Temperature distribution of asphalt mastics via using infrared cameras.

As suggested in **Fig. 8a**, all mastics' temperature increases with longer durations of microwave radiation. Specifically, the AM-LP sample exhibits a gradual increase in temperature with extended microwave durations, reaching 54.4℃ at 180 seconds. Comparatively, the surface temperature of the AM-CGP, AM-

FP, and AM-FA samples increases by 25-50℃, 50-80℃, and 10-40℃, respectively, in comparison to the AM-LP samples, suggesting that introducing microwave-sensitive fillers can improve the microwave heating capacity of asphalt materials due to the high content of metal oxide components in these fillers, which enhance their ability to absorb microwaves. Notably, both the AM-CGP and AM-FP samples achieve average surface temperatures exceeding 95℃ at 60 seconds of heating. Consequently, 60 seconds of radiation is used to compare the microwave heating capacities of these specimens. Additionally, the heating rates for the AM-CGP, AM-FP, and AM-FA samples are calculated to be 0.52℃/s, 0.65℃/s, and 0.39℃/s, respectively (as illustrated in **Fig. 8b**). These values are higher than that of the AM-LP specimen, which is 0.16℃/s. It should be noted that the heating rate and temperature of the asphalt materials can be adjusted by optimizing microwave parameters, taking into account the softening point of the asphalt.

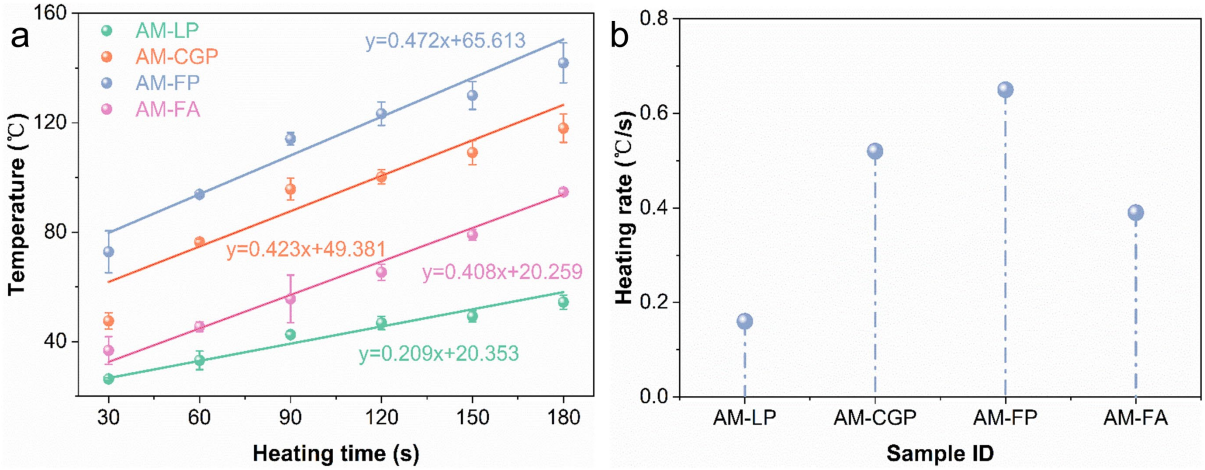

Fig. 8. Microwave heating of asphalt mastics: (a) surface temperature and (b) heating rate.

3.4. Initial self-healing temperature of asphalt mastics

The complex viscosity of all asphalt mastics displays a decreasing trend as the scanning frequency and temperature increase (**Fig. 9**). Notably, at higher temperatures, particularly at 85℃ and 100℃, the curves become horizontal lines, indicating that the complex viscosity of asphalt mastics remains relatively constant with varying frequencies. This observation suggests that the flow behavior of asphalt mastics is highly influenced by temperature and is close to a near-Newtonian fluid, as stated by Garcia et al. (García, 2012). To assess the changes in asphalt flow performance, the temperature frequency scanning test was performed. **Fig. 10** summarises the flow characteristics of the asphalt mastics.

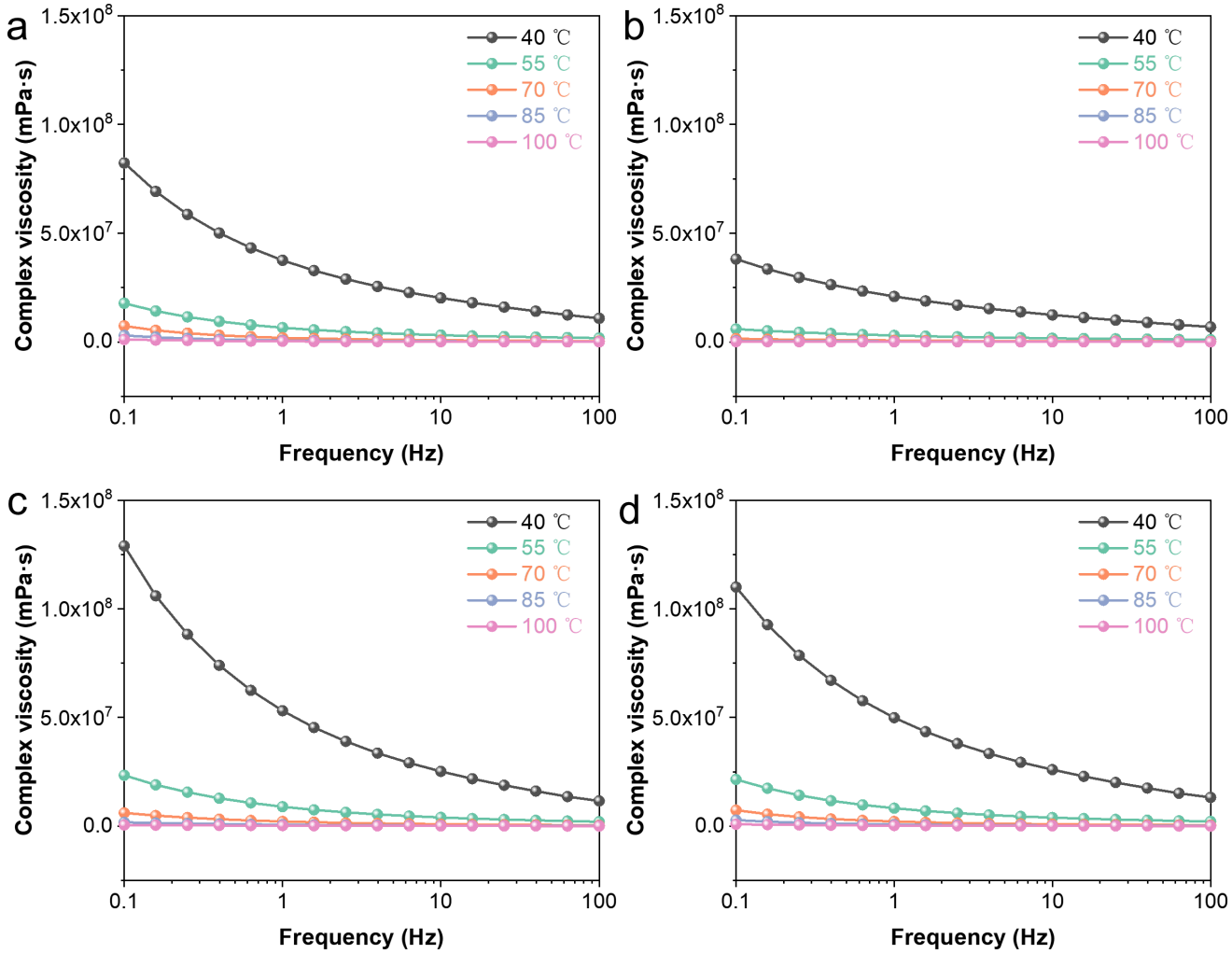

Fig. 9. The function of scanning frequency and complex viscosity of asphalt mastics: (a) AM-LP sample; (b) AM-CGP sample; (c) AM-FP sample; and (d) AM-FA sample.

The results presented in **Fig. 10** show the fitting outcomes for the flow behavior indexes of asphalt mastics at different temperatures. The flow behavior indexes of all samples increase with the increasing temperature, and the increasing tendency becomes slower at higher temperatures. Especially, the gaps in flow behavior indexes among the asphalt mastics samples become less significant, mainly ascribed to the asphalt mastic beginning to resemble a Newtonian liquid as its flow behavior index over 0.9, where the flow state of the asphalt mastics tends to be unchanged. Based on the fitting results, the initial self-healing temperature value for the AM-LP sample is determined to be 88.2°C. In contrast, the initial self-healing temperatures of the microwave-sensitive fillers modified asphalt mastics decrease to 81.1°C (AM-FA sample), 65.6°C (AM-CGP sample), and 56.2°C (AM-FP sample), respectively. This suggests that the AM-LP sample needs a higher temperature to reach a similar flow state relative to the microwave-sensitive

fillers modified asphalt mastics. Consequently, using microwave-sensitive fillers can enable asphalt materials to achieve substantial microwave-heating healing efficiency at lower energy consumption.

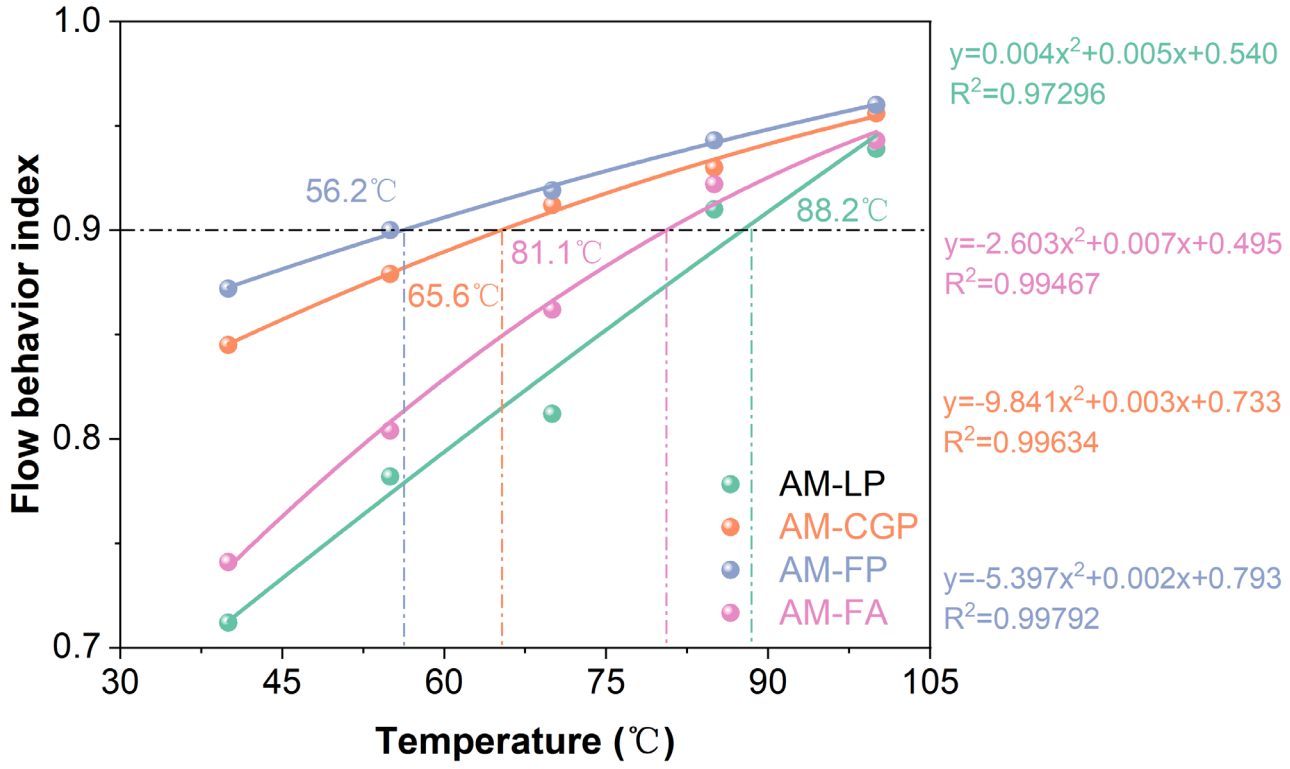

Fig. 10. Flow behavior index of asphalt mastics.

3.5. Microwave-heating healing capability of asphalt mixture

In this section, the microwave-heating healing behavior of asphalt materials is evaluated using PA-13 mixtures. The results obtained from the microwave heating characteristics and flow behavior indexes indicate that FA has limited potential to enhance the heating-healing efficiency of asphalt composites. As a result, it is excluded from further analysis in this section. **Fig. 11a** presents the mixture's initial force and the forces of the mixtures after three damage-healing-damage cycles. It is important to note that each group of samples undergoes triple repetition tests, and one random sample from each group is displayed in the figure. Additionally, the peak force of all mixtures decreases with increasing the damage-healing cycle. Interestingly, the peak forces of the LP-modified mixtures and FP-modified mixtures samples significantly exceed the LP-modified mixtures.

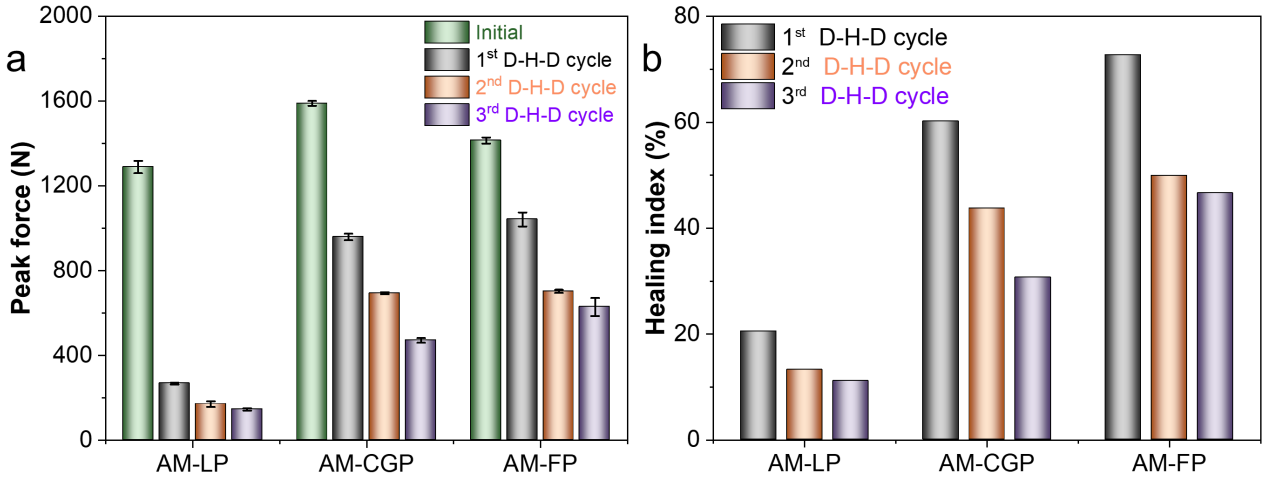

Fig. 11. Healing efficiency of asphalt mixtures (AM): (a) peak force and (b) the calculated HI values. D-H-D is damage-healing-damage.

The HI is calculated to further assess the healing efficiency of asphalt composites, as presented in **Fig. 11b**. As suggested in **Fig. 11b**, the AM-LP's HI achieves 20.5% at the initial state and its HI decreases to 11.1% after three damage-healing-damage cycles, indicating poor heating-healing capability. Remarkably, asphalt mixtures incorporating microwave-sensitive fillers demonstrate higher HI relative to the AM-LP specimens, implying an increased heating-healing efficiency compared to the AM-LP specimens, indicating that substituting LP with CGP or FP can increase the healing efficiency of the mixture, as CGP or FP possess outstanding microwave absorption ability, which aligns with the surface temperature results of the asphalt materials. Furthermore, the AM-CGP and AM-FP samples achieve HI values of 30.7% and 46.6% after three damage-healing cycles, respectively, indicating that FP-modified asphalt mixtures perform better in enhancing the microwave-heating healing capability compared to using CGP. Note that the HI values of the AM-CGP and AM-FP samples are below 50% after three damage-healing cycles. To further enhance the heating-healing efficiency of the asphalt composites, it would be ideal to explore and investigate the combined usage of functional fillers and functional aggregates, which will be addressed in future studies.

4. Environmental benefits and economic cost (EBEC) analysis

This section undertakes a comparative evaluation of the environmental benefits and economic costs (EBEC) associated with two types of pavement: conventional pavement (LP-modified asphalt mixtures) and self-healing pavement (FP-modified asphalt mixtures). The analysis focuses on the unit pavement of PA-13 asphalt mixture, which has dimensions of 1000 m in length and 3.75 m in width. To evaluate the

effectiveness of the self-healing pavement, key parameters such as the microwave heating ratio (MHR) and energy conversion improvement rate (ECIR) are determined. These parameters are calculated utilizing **Equation** (4), resulting in an MHR value of 0.65°C/s and an ECIR value of 3.063. **Equation** (5) is employed to quantify the amount of electric energy saved on the pavement. Subsequently, a conversion is made to estimate the energy savings experienced by the pavement based on the percentage of area, considering the electric energy saved by the specimen. At last, the economic cost of the unit pavement is determined by utilizing **Equation** (6) and **Equation** (7).

$$ECIR=(M_{HRN}-M_{HRC})/M_{HRC} \quad (4)$$

$$W_{Specimen}=P_{Microwave}\times t\times ECIR \quad (5)$$

$$W_{Pavement}=W_{Specimen}\times S_{Ratio} \quad (6)$$

$$EF_{Pavement}=W_{Pavement}\times 1.0 \quad (7)$$

where M_{HRN} and M_{HRC} are the MHR of self-healing asphalt material and conventional asphalt material (°C/s), respectively. $W_{Specimen}$ and $P_{Microwave}$ are the electric energy saved by the specimen (kW·h) and the microwave power (800 W); t is the microwave radiation duration (3 minutes); S_{Ratio} is the percentage of the area between specimen and unit pavement; $W_{Specimen}$ and $EF_{Pavement}$ are the electric energy saved (kW·h) and electric costs saved by unit pavement (USD), and the local electricity price is about 0.15 USD/kW·h.

Global warming has emerged as a significant and pressing issue across the globe since the 1980s (Abdalla et al., 2022; Deng et al., 2023; Fanijo et al., 2023). Carbon dioxide (CO_2) is the main contributor to the greenhouse effect, accounting for about 55% of the overall greenhouse effect (Fu et al., 2022). China, being predominantly reliant on thermal power generation, faces challenges due to CO_2 emissions resulting from the combustion of raw coal. Consequently, the greenhouse effect in China is aggravated (Fu et al., 2023). Pavement engineering is known for being a high-energy and high-carbon activity (Lu et al., 2023f), and the carbon footprint is further increased by the need for frequent maintenance activities (Jiang, X. et al., 2023; Ma et al., 2023; Ma et al., 2022a). To address this issue, this study mainly analyses the self-healing pavement and its potential contribution to reducing CO_2 emissions. Specifically, the environmental benefits associated with the unit pavement are assessed by examining CO_2 emissions. This analysis involves several steps:

1) Assessment of the consumed power in terms of the microwave power cost converted into calorific

385 value.

386 2) Calculation of the amount of raw coal required to yield the calorific value.

387 3) Evaluation of the CO_2 emissions during the microwave heating-healing process based on the CO_2
388 emission coefficient of raw coal.

389 **Equation** (8) and **Equation** (9) are employed to determine the amount of calorific value saved by the
390 pavement and the quality of raw coal, respectively.

391 $$Q_{\text{Specimen}}=W_{\text{Specimen}}\times 3.6\times 1000 \quad (8)$$

392 $$M_{\text{Raw coal}}=Q_{\text{Specimen}}/Q_{\text{Raw coal}} \quad (9)$$

393 where Q_{Specimen} is the calorific value saved by pavement (kJ); $M_{\text{Raw coal}}$ is the content of raw coal (kg);
394 $Q_{\text{Raw coal}}$ is the calorific value of 1 kg of raw coal (kJ/kg). At last, the amount of CO_2 emissions can be
395 calculated using **Equation** (10).

396 $$V_{CO_2}=M_{\text{Raw coal}}\times C_{CO_2} \quad (10)$$

397 where V_{CO_2} and C_{CO_2} are the amounts of CO_2 emissions (kg) and CO_2 emission coefficient of raw coal,
398 respectively.

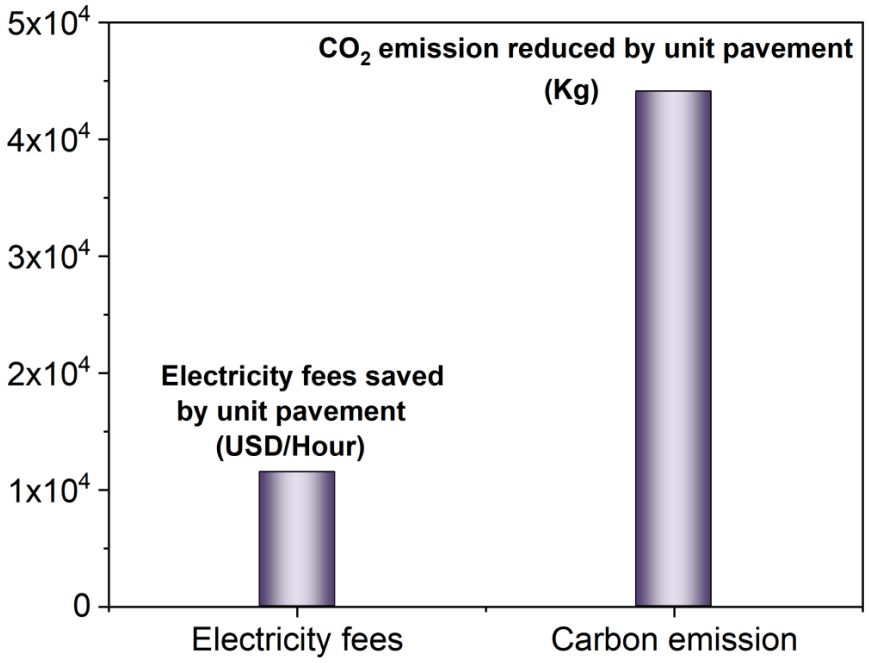

Fig. 12. Calculated electricity savings and reduced CO_2 emissions per unit of pavement.

According to the aforementioned analysis, it is evident that microwave-heating healing asphalt pavement offers substantial advantages in terms of reducing CO_2 emissions compared to conventional pavement. As demonstrated in **Fig. 12**, the unit pavement achieves notable outcomes in terms of both cost savings and CO_2 emission reduction. Specifically, the electric fees saved amount to 1.15×10^4 USD, while the corresponding reduction in CO_2 emissions is estimated to be 4.41×10^4 kg. These results unequivocally highlight the exceptional EBEC benefits associated with the implementation of microwave-heating healing PA-13 pavement.

5. Findings and summary

In this study, three microwave-sensitive fillers, namely, coal gangue powder (CGP), ferrite powder (FP), and fly ash (FA), were recycled as alternatives to limestone powder (LP) filler to create microwave-heating healing asphalt materials with enhanced sustainability. The incorporation of these fillers resulted in significant improvements in key properties of the asphalt materials, including resistance to rutting, microwave heating capacity, and effectiveness in microwave-heating healing. The outcomes and analysis of this research led to the following findings:

(1) The microwave-sensitive fillers have higher electromagnetic parameters than that of the LP filler, which allows them to convert microwave irradiation into thermal energy more efficiently when incorporated into asphalt materials. This leads to improved microwave heating ability and heating-healing capability in the asphalt materials, making them highly promising for such applications compared to those containing LP filler. Notably, both AM-CGP and AM-FP mastics achieve average surface temperatures above 95℃ within just 60 seconds.

(2) In the AM-LP sample, the initial self-healing temperature is approximately 88°C. However, by incorporating microwave-sensitive fillers, the asphalt mastics exhibit lower initial self-healing temperatures: 81°C for AM-FA, 66°C for AM-CGP, and 56°C for AM-FP. This suggests that the presence of microwave-sensitive fillers allows the asphalt composites to achieve a flow state at lower temperatures compared to AM-LP. As a result, the heating-healing efficiency of the asphalt materials can be improved and energy consumption can be reduced.

(3) The asphalt mixtures modified with CGP filler and FP filler achieve healing indexes (HI) of 31% and 47% respectively after three cycles of damage-healing-damage. These results indicate that FP-modified asphalt mixtures outperform CGP-modified mixtures in terms of enhancing microwave-heating healing

ability. However, the HI values remain below 50% even after three cycles, suggesting that the use of CGP or FP filler alone is not sufficient to significantly enhance the healing efficiency of asphalt mixtures. One possible reason for this limitation is the limited volume of filler in the mixtures. In future studies, it is recommended to explore and investigate the combination of functional fillers and functional aggregates as a more promising strategy to increase the microwave-heating healing efficiency of asphalt mixtures.

(4) The analysis of environmental benefits and economic costs reveals that the adoption of asphalt mixture modified with microwave-sensitive fillers can result in significant savings in electricity costs, estimated at 1.15×10^4 USD. Furthermore, this implementation is projected to lead to a reduction of approximately 4.41×10^4 kg in CO_2 emissions. These promising findings provide a robust basis for the practical application of asphalt mixture incorporating microwave-sensitive fillers.

Acknowledgments

The authors would like to express their sincere gratitude for the financial support received from the Hong Kong Research Grant Council through the GRF Project 15209920 and GRF Project 15220621. Additionally, the authors acknowledge the Start-up Fund for RAPs under the Strategic Hiring Scheme (P0048182) from PolyU (UGC). The funding received greatly contributed to the successful completion of this research project. The authors would also like to thank Mr. Paul Choi and Dr. Zhifei Tan for their assistance in sample preparation and testing.

References

Abdalla, A., Faheem, A.F., Alsalihi, M., Sobolev, K., 2022. Investigation of the influence of Off-Spec coal combustion waste on asphalt binder rheological performance and aging sensitivity. Cleaner Materials 4.http://dx.doi.org/10.1016/j.clema.2022.100073

Amani, S., Kavussi, A., Karimi, M.M., 2020. Effects of aging level on induced heating-healing properties of asphalt mixes. Construction and Building Materials 263.http://dx.doi.org/10.1016/j.conbuildmat.2020.120105

Anupam, B.R., Sahoo, U.C., Chandrappa, A.K., 2022. A methodological review on self-healing asphalt pavements. Construction and Building Materials 321.http://dx.doi.org/10.1016/j.conbuildmat.2022.126395

Deng, Z., Li, W., Dong, W., Sun, Z., Kodikara, J., Sheng, D., 2023. Multifunctional asphalt concrete pavement toward smart transport infrastructure: Design, performance and perspective. Composites Part B: Engineering.http://dx.doi.org/10.1016/j.compositesb.2023.110937

Fanijo, E.O., Kolawole, J.T., Babafemi, A.J., Liu, J., 2023. A comprehensive review on the use of recycled concrete aggregate for pavement construction: Properties, performance, and sustainability. Cleaner Materials

9.http://dx.doi.org/10.1016/j.clema.2023.100199

Fu, C., Liu, K., Liu, P., Oeser, M., 2022. Experimental and numerical investigation of magnetic converge effect of magnetically conductive asphalt mixture. Construction and Building Materials 360.http://dx.doi.org/10.1016/j.conbuildmat.2022.129626

Fu, C., Liu, K., Liu, Q., Xu, P., Dai, D., Tong, J., 2023. Exploring directional energy conversion behavior of electromagnetic-based multifunctional asphalt pavement. Energy 268.http://dx.doi.org/10.1016/j.energy.2022.126573

García, Á., 2012. Self-healing of open cracks in asphalt mastic. Fuel 93, 264-272.http://dx.doi.org/10.1016/j.fuel.2011.09.009

García, A., Bueno, M., Norambuena-Contreras, J., Partl, M.N., 2013. Induction healing of dense asphalt concrete. Construction and Building Materials 49, 1-7.http://dx.doi.org/10.1016/j.conbuildmat.2013.07.105

Grossegger, D., Garcia, A., 2019. The effect of water and pressure on the self-healing of macro cracks in asphalt mortar beams. Construction and Building Materials 229.http://dx.doi.org/10.1016/j.conbuildmat.2019.116941

Guan, B., Liu, J., Zhao, H., Wu, J., Liu, J., Yang, F., 2019. Investigation of the Microwave Absorption of Asphalt Mixtures Containing Magnetite Powder. Coatings 9(12).http://dx.doi.org/10.3390/coatings9120813

Hong, R.-b., Wu, J.-r., Cai, H.-b., 2020. Low-temperature crack resistance of coal gangue powder and polyester fibre asphalt mixture. Construction and Building Materials 238.http://dx.doi.org/10.1016/j.conbuildmat.2019.117678

Jahanbakhsh, H., Karimi, M.M., Jahangiri, B., Nejad, F.M., 2018. Induction heating and healing of carbon black modified asphalt concrete under microwave radiation. Construction and Building Materials 174, 656-666.http://dx.doi.org/10.1016/j.conbuildmat.2018.04.002

Jiang, Q., Liu, W., Wu, S., 2023. Analysis on factors affecting moisture stability of steel slag asphalt concrete using grey correlation method. Journal of Cleaner Production 397.http://dx.doi.org/10.1016/j.jclepro.2023.136490

Jiang, X., Zhu, H., Yan, Z., Zhang, F., Ye, F., Li, P., Zhang, X., Dai, Z., Bai, Y., Huang, B., 2023. A state-of-art review on development and progress of backfill grouting materials for shield tunneling. Developments in the Built Environment 16.http://dx.doi.org/10.1016/j.dibe.2023.100250

Jiang, Y., Ling, T.-C., Shi, C., Pan, S.-Y., 2018. Characteristics of steel slags and their use in cement and concrete—A review. Resources, Conservation and Recycling 136, 187-197.http://dx.doi.org/10.1016/j.resconrec.2018.04.023

Karimi, M.M., Amani, S., Jahanbakhsh, H., Jahangiri, B., Alavi, A.H., 2021. Induced heating-healing of conductive asphalt concrete as a sustainable repairing technique: A review. Cleaner Engineering and Technology 4.http://dx.doi.org/10.1016/j.clet.2021.100188

Karimi, M.M., Jahanbakhsh, H., Jahangiri, B., Moghadas Nejad, F., 2018. Induced heating-healing characterization of activated carbon modified asphalt concrete under microwave radiation. Construction and Building Materials 178, 254-271.http://dx.doi.org/10.1016/j.conbuildmat.2018.05.012

Li, C., Wu, S., Chen, Z., Tao, G., Xiao, Y., 2018. Enhanced heat release and self-healing properties of steel slag filler based

asphalt materials under microwave irradiation. Construction and Building Materials 193, 32-41.http://dx.doi.org/10.1016/j.conbuildmat.2018.10.193

Li, F., Zhao, X., Zhang, X., 2023. Utilizing original and activated coal gangue wastes as alternative mineral fillers in asphalt binder: Perspectives of rheological properties and asphalt-filler interaction ability. Construction and Building Materials 365.http://dx.doi.org/10.1016/j.conbuildmat.2022.130069

Li, J., Cao, Y., Sha, A., Song, R., Li, C., Wang, Z., 2022. Prospective application of coal gangue as filler in fracture-healing behavior of asphalt mixture. Journal of Cleaner Production 373.http://dx.doi.org/10.1016/j.jclepro.2022.133738

Liu, J., Hao, P., Dou, Z., Wang, J., Ma, L., 2021. Rheological, healing and microstructural properties of unmodified and crumb rubber modified asphalt incorporated with graphene/carbon black composite. Construction and Building Materials 305.http://dx.doi.org/10.1016/j.conbuildmat.2021.124512

Liu, J., Wang, Z., Jia, H., Jing, H., Chen, H., Zhou, L., Yuan, L., Hoff, I., 2023. Characteristics and properties of asphalt mortar containing FO filler. Construction and Building Materials 392.http://dx.doi.org/10.1016/j.conbuildmat.2023.132039

Liu, J., Wang, Z., Li, M., Wang, X., Wang, Z., Zhang, T., 2022. Microwave heating uniformity, road performance and internal void characteristics of steel slag asphalt mixtures. Construction and Building Materials 353.http://dx.doi.org/10.1016/j.conbuildmat.2022.129155

Liu, Q., Wu, S., Schlangen, E., 2013. Induction heating of asphalt mastic for crack control. Construction and Building Materials 41, 345-351.http://dx.doi.org/10.1016/j.conbuildmat.2012.11.075

Lou, B., Liu, Z., Sha, A., Jia, M., Li, Y., 2020. Microwave Absorption Ability of Steel Slag and Road Performance of Asphalt Mixtures Incorporating Steel Slag. Materials (Basel) 13(3).http://dx.doi.org/10.3390/ma13030663

Lu, D., Jiang, X., Leng, Z., Huo, Y., Wang, D., Zhong, J., 2023a. Electrically conductive asphalt concrete for smart and sustainable pavement construction: A review. Construction and Building Materials 406.http://dx.doi.org/10.1016/j.conbuildmat.2023.133433

Lu, D., Jiang, X., Leng, Z., Zhang, S., Wang, D., Zhong, J., 2023b. Dual responsive microwave heating-healing system in asphalt concrete incorporating coal gangue and functional aggregate. Journal of Cleaner Production 422.http://dx.doi.org/10.1016/j.jclepro.2023.138648

Lu, D., Jiang, X., Tan, Z., Yin, B., Leng, Z., Zhong, J., 2023c. Enhancing sustainability in pavement Engineering: A-state-of-the-art review of cement asphalt emulsion mixtures. Cleaner Materials 9.http://dx.doi.org/10.1016/j.clema.2023.100204

Lu, D., Leng, Z., Lu, G., Wang, D., Huo, Y., 2023d. A critical review of carbon materials engineered electrically conductive cement concrete and its potential applications. International Journal of Smart and Nano Materials, 1-27.http://dx.doi.org/10.1080/19475411.2023.2199703

Lu, D., Sheng, Z., Yan, B., Jiang, Z., Wang, D., Zhong, J., 2023e. Rheological Behavior of Fresh Cement Composites with

519 Graphene Oxide–Coated Silica Fume. Journal of Materials in Civil Engineering 35(10).http://dx.doi.org/10.1061/jmcee7.Mteng-
520 15428
521 Lu, D., Wang, D., Wang, Y., Zhong, J., 2023f. Nano-engineering the interfacial transition zone between recycled concrete
522 aggregates and fresh paste with graphene oxide. Construction and Building Materials
523 384.http://dx.doi.org/10.1016/j.conbuildmat.2023.131244
524 M. Karimi, M., Ahmadi Dehaghi, E., Behnood, A., 2022. Cracking features of asphalt mixtures under induced heating-healing.
525 Construction and Building Materials 324.http://dx.doi.org/10.1016/j.conbuildmat.2022.126625
526 Ma, Y., Wang, S., Zhang, M., Jiang, X., Polaczyk, P., Huang, B., 2023. Weather aging effects on modified asphalt with rubber-
527 polyethylene composites. Sci Total Environ 865, 161089.http://dx.doi.org/10.1016/j.scitotenv.2022.161089
528 Ma, Y., Wang, S., Zhou, H., Hu, W., Polaczyk, P., Huang, B., 2022a. Recycled polyethylene and crumb rubber composites
529 modified asphalt with improved aging resistance and thermal stability. Journal of Cleaner Production
530 334.http://dx.doi.org/10.1016/j.jclepro.2021.130102
531 Ma, Y., Zheng, K., Ding, Y., Polaczyk, P., Jiang, X., Huang, B., 2022b. Binder availability and blending efficiency of reclaimed
532 asphalt: A state-of-the-art review. Construction and Building Materials
533 357.http://dx.doi.org/10.1016/j.conbuildmat.2022.129334
534 Ma, Y., Zhou, H., Jiang, X., Polaczyk, P., Xiao, R., Zhang, M., Huang, B., 2021. The utilization of waste plastics in asphalt
535 pavements: A review. Cleaner Materials 2.http://dx.doi.org/10.1016/j.clema.2021.100031
536 Mehrara, A., Khodaii, A., 2015. Quantification of damage recovery of asphalt concrete as a consequence of rest time application
537 using dissipated energy. Materials and Structures 49(7), 2947-2960.http://dx.doi.org/10.1617/s11527-015-0697-0
538 Meng, Y., Lai, J., Ling, L., Zhang, C., Chen, J., Zhu, J., 2023. Preparation of an eco-friendly de-icing filler and its effects on the
539 performance of different asphalt mastic. Construction and Building Materials
540 364.http://dx.doi.org/10.1016/j.conbuildmat.2022.129967
541 Muhammad, J., Peng, T., Zhang, W., Cheng, H., Waqas, H., Abdul, S., Chen, K., Zhou, Y., 2021. Moisture susceptibility and
542 fatigue performance of asphalt binder modified by bone glue and coal fly ash. Construction and Building Materials
543 308.http://dx.doi.org/10.1016/j.conbuildmat.2021.125135
544 Nabiun, N., Khabiri, M.M., 2016. Mechanical and moisture susceptibility properties of HMA containing ferrite for their use in
545 magnetic asphalt. Construction and Building Materials 113, 691-697.http://dx.doi.org/10.1016/j.conbuildmat.2016.03.058
546 Norambuena-Contreras, J., Garcia, A., 2016. Self-healing of asphalt mixture by microwave and induction heating. Materials &
547 Design 106, 404-414.http://dx.doi.org/10.1016/j.matdes.2016.05.095
548 Santero, N.J., Masanet, E., Horvath, A., 2011. Life-cycle assessment of pavements. Part I: Critical review. Resources,
549 Conservation and Recycling 55(9-10), 801-809.http://dx.doi.org/10.1016/j.resconrec.2011.03.010

Schuster, L., Staub de Melo, J.V., Villena Del Carpio, J.A., 2023. Effects of the associated incorporation of steel wool and carbon nanotube on the healing capacity and mechanical performance of an asphalt mixture. International Journal of Fatigue 168.http://dx.doi.org/10.1016/j.ijfatigue.2022.107440

Segundo, I.R., Freitas, E., Branco, V.T.F.C., Landi, S., Costa, M.F., Carneiro, J.O., 2021. Review and analysis of advances in functionalized, smart, and multifunctional asphalt mixtures. Renewable and Sustainable Energy Reviews 151.http://dx.doi.org/10.1016/j.rser.2021.111552

Song, Q., Guo, M.-Z., Wang, L., Ling, T.-C., 2021. Use of steel slag as sustainable construction materials: A review of accelerated carbonation treatment. Resources, Conservation and Recycling 173.http://dx.doi.org/10.1016/j.resconrec.2021.105740

Song, W., Deng, Z., Wu, H., Xu, Z., 2023a. Cohesive zone modeling of I–II mixed mode fracture behaviors of hot mix asphalt based on the semi-circular bending test. Theoretical and Applied Fracture Mechanics 124.http://dx.doi.org/10.1016/j.tafmec.2023.103781

Song, W., Xu, Z., Xu, F., Wu, H., Yin, J., 2021. Fracture investigation of asphalt mixtures containing reclaimed asphalt pavement using an equivalent energy approach. Engineering Fracture Mechanics 253.http://dx.doi.org/10.1016/j.engfracmech.2021.107892

Song, W., Zou, X., Wu, H., Yang, F., 2023b. Energy evolution in fracture process of hot mix asphalt containing reclaimed asphalt pavement and rejuvenator. Theoretical and Applied Fracture Mechanics 124.http://dx.doi.org/10.1016/j.tafmec.2023.103809

Tan, Y., Shan, L., Richard Kim, Y., Underwood, B.S., 2012. Healing characteristics of asphalt binder. Construction and Building Materials 27(1), 570-577.http://dx.doi.org/10.1016/j.conbuildmat.2011.07.006

Varma, R., Balieu, R., Kringos, N., 2021. A state-of-the-art review on self-healing in asphalt materials: Mechanical testing and analysis approaches. Construction and Building Materials 310.http://dx.doi.org/10.1016/j.conbuildmat.2021.125197

Wan, P., Liu, Q., Wu, S., Zou, Y., Zhao, F., Wang, H., Niu, Y., Ye, Q., 2022. Dual responsive self-healing system based on calcium alginate/Fe3O4 capsules for asphalt mixtures. Construction and Building Materials 360.http://dx.doi.org/10.1016/j.conbuildmat.2022.129585

Wang, H., Yang, J., Liao, H., Chen, X., 2016. Electrical and mechanical properties of asphalt concrete containing conductive fibers and fillers. Construction and Building Materials 122, 184-190.http://dx.doi.org/10.1016/j.conbuildmat.2016.06.063

Wang, Y., Polaczyk, P., He, J., Lu, H., Xiao, R., Huang, B., 2022. Dispersion, compatibility, and rheological properties of graphene-modified asphalt binders. Construction and Building Materials 350.http://dx.doi.org/10.1016/j.conbuildmat.2022.128886

Wen, S., Chung, D.D.L., 2004. Effects of carbon black on the thermal, mechanical and electrical properties of pitch-matrix composites. Carbon 42(12-13), 2393-2397.http://dx.doi.org/10.1016/j.carbon.2004.04.005

Woszuk, A., Bandura, L., Franus, W., 2019. Fly ash as low cost and environmentally friendly filler and its effect on the properties

581 of mix asphalt. Journal of Cleaner Production 235, 493-502.http://dx.doi.org/10.1016/j.jclepro.2019.06.353
582 Xu, S., García, A., Su, J., Liu, Q., Tabaković, A., Schlangen, E., 2018. Self-Healing Asphalt Review: From Idea to Practice.
583 Advanced Materials Interfaces 5(17).http://dx.doi.org/10.1002/admi.201800536
584 Yang, C., Wu, S., Cui, P., Amirkhanian, S., Zhao, Z., Wang, F., Zhang, L., Wei, M., Zhou, X., Xie, J., 2022a. Performance
585 characterization and enhancement mechanism of recycled asphalt mixtures involving high RAP content and steel slag. Journal
586 of Cleaner Production 336.http://dx.doi.org/10.1016/j.jclepro.2022.130484
587 Yang, C., Wu, S., Xie, J., Amirkhanian, S., Liu, Q., Zhang, J., Xiao, Y., Zhao, Z., Xu, H., Li, N., Wang, F., Zhang, L., 2022b.
588 Enhanced induction heating and self-healing performance of recycled asphalt mixtures by incorporating steel slag. Journal of
589 Cleaner Production 366.http://dx.doi.org/10.1016/j.jclepro.2022.132999
590 Zhou, X., Wang, Z., Wang, X., Guo, H., Ji, X., Liu, J., 2022. Utilization of calcium carbide slag as alternative filler in asphalt
591 mastic: Filler characteristics, rheological and adhesion properties. Journal of Cleaner Production
592 380.http://dx.doi.org/10.1016/j.jclepro.2022.134980
593 Zhu, X., Ye, F., Cai, Y., Birgisson, B., Lee, K., 2019. Self-healing properties of ferrite-filled open-graded friction course (OGFC)
594 asphalt mixture after moisture damage. Journal of Cleaner Production 232, 518-
595 530.http://dx.doi.org/10.1016/j.jclepro.2019.05.353
596